PHYSICAL REVIEW E VOLUME 52, NUMBER 6 DECEMBER 1995

Generalized monomer-monomer model for catalysis

Eric Clément
Laboratoire d'Acoustique et d'Optique et de la Matière Condensée, Université Pierre et Marie Curie, 4 place Jussieu-B86, 75005 Paris, France

Patrick Leroux-Hugon
Groupe de Physique du Solide, Université Denis Diderot, 2 place Jussieu, 75005 Paris, France

Leonard M. Sander
Department of Physics, The University of Michigan, Ann Arbor, Michigan 48109

(Received 18 July 1995)

We consider a Langmuir-Hinshelwood reaction on a catalytic surface with two monomer reactants A and B whose reaction product leaves the surface: $A + B \to 0$. We allow different adsorption and desorption rates for the two reactants. When adsorption and reaction are fast events compared to desorption (and in the absence of diffusion), we can use an approximate mapping onto a two-state spin model that we solve using a decoupling scheme. We compute the steady-state reaction rate and compare it to Monte Carlo simulations. We show explicitly how spatial fluctuations affect the behavior and that the predictions of the spin model give a reasonable theory for the system.

PACS number(s): 05.40.+j, 82.65.Jv, 05.45.+b

I. INTRODUCTION

Though catalytically activated processes have been known for a very long time, there are still phenomena in the field that remain a challenge for fundamental research. One of the most active areas is the study of collective effects, such as fluctuations and spatial organization of reactants, as opposed to the traditional approach, which focuses on local energetic considerations. There is now a large literature on models that include stochastic effects in catalysis [1,2]. These are intended to investigate fluctuations and correlations. One of the best known examples is the simple monomer-dimer model of Ziff *et al.* [1] for the catalysis of CO_2.

A still simpler stochastic model which nevertheless shows many fascinating statistical effects was proposed by Fichthorn, Gulari, and Ziff (FGZ) [2]. It considers a system with two monomer species on a surface which react and annihilate when they encounter one another, i.e., $A+B \to 0$. The particles are assumed to adsorb and desorb with rates that are the same for the two species. The system is reaction-limited: any empty sites are immediately filled. The reaction-limited symmetric FGZ model was solved exactly by Clément, Leroux-Hugon, and Sander [3] on any Euclidean lattice, and an extension of the solution to disordered lattices has been proposed by Clément, Leroux-Hugon, and Argyrakis [4]. Kapivski [5] and also Flament *et al.* [6] have solved a related dynamical problem This monomer-monomer model has also been considered by Evans and Ray [7].

Here we extend the FGZ model to the situation where the two desorption and adsorption rates are different, and we allow for the possibility that not all sites are filled. We will find many interesting features for this generalized model. In a limiting case, i.e., when the surface is covered by the two species, we propose an analysis based on our previous solution. This involves a two-state spin model. This model is solved using a decoupling approximation at the three-particle correlation level. We compare these results to a mean-field (MF) solution. We show, in contrast to MF predictions that there is an important dependence on dimensionality, and we give a scaling argument that extends the results to fractal structures. We will test our predictions by doing Monte Carlo simulations.

Albano [8] considered the dynamics of a special case of our model showing a Schlögl second order transition [9]. He did simulations on a percolation cluster to test for a possible new universality class and found a new exponent. This has been disputed by Zhuo and Redner [10] who claim that the model should be in the well-known class of directed percolation, since there is a transition to a single absorbing state [12].

In the next section we introduce the model and work out the MF theory. Then we give our solution to the spin model. In the last section we compare Monte Carlo simulations to our approximate solution.

II. GENERALIZED REACTION MODEL

A. Description

Consider two different species A and B absorbed on a catalytic surface that is a d-dimensional lattice. We consider a reaction scheme of the Langmuir-Hinshelwood type with three steps:

Adsorption: [(probability)/(time)]/(site), P_A, P_B:

$$A^* + [x] \to A \ ,$$
$$B^* + [x] \to B.$$

Desorption: [(probability)/(time)]/(site), P^d_A, P^d_B:

$$A \rightarrow [x] + A^* \ ,$$
$$B \rightarrow [x] + B^*.$$

Reaction:

$$A + B \rightarrow [x] + [x] + AB^*.$$

The probabilities, $P_{A,B}, P^d_{A,B}$ are parameters in the model. The symbol $*$ means a species in the gas phase and $[x]$ means a free site. We assume a fast time scale for the reaction and even a faster one for the adsorption. Since there is no diffusion we are free to use the reaction rate to define the time scale. The different feature of this model as compared to FGZ is the asymmetry of the rates $P_{A,B}$ and $P^d_{A,B}$. To parametrize this we introduce a set of three variables (x, y, p), where $P_A = (1-x)/2$, $P_B = (1+x)/2$, $P^d_A = p(1+y)/2$, $P^d_B = p(1-y)/2$. The FGZ model is recovered by making $P_A = P_B = 1/2$ and $P^d_A = P^d_B$, i.e., $x = y = 0$. The lattice is a regular d-dimensional quadratic lattice with $N = L^d$ lattice sites and coordination number $2d$.

The model we propose here may appear too simple to give any insight into real catalysis. However, despite its simplicity it has rather unusual collective effects that could occur in the real world, and which might be missed in the context of a more complicated system. Specifically, our model shows interesting behavior as the result of confinement and geometrical disorder, which are complications very commonly encountered in surface science.

B. Mean-field theory

A preliminary report on Monte Carlo simulations of this model [11] illustrated anomalous behavior for the reaction rate. Below we derive an expression showing explicitly how classical chemical kinetics fails. In this section, however, we consider the classical MF theory.

In MF reaction kinetics, the reaction rate is the product of the reactant concentrations. This assumption does not consider any of the spatial correlations that may occur at a mesoscopic level on the substrate [11]. In MF our reaction model is described by the following set of nonlinear coupled equations:

$$d\rho_A/dt = -k\rho_A\rho_B + P_A(1-\rho_A-\rho_B) - P^d_A\rho_A \ ,$$
$$d\rho_B/dt = -k\rho_A\rho_B + P_B(1-\rho_A-\rho_B) - P^d_B\rho_B \ , \qquad (1)$$

where ρ_A, ρ_B are, respectively, the densities of A and B, and where k represents the probability/time of reaction when two species are in contact. We take k to be a number of the order of unity. We will use variables $\rho = \rho_A + \rho_B$, the total coverage; $\gamma = \rho_A - \rho_B$, the difference concentration; and $Q = k\rho_A\rho_B$, the reaction rate.

In the steady state, the solution is easy to write:

$$\gamma = \frac{4xQ}{p(1+xy)} - \rho\frac{x+y}{p(1+xy)} \ , \qquad (2)$$

$$\rho = \frac{1-2Q+px\gamma/2}{p(1+p/2)} \ , \qquad (3)$$

$$Q = \frac{k}{4}(\rho^2-\gamma^2) \ . \qquad (4)$$

The total coverage obeys a quadratic equation, $a\rho^2 - b\rho + c = 0$, where $u = x/p$ is a reduced variable and the coefficients of the quadratic equation are

$$a(u,y) = \frac{k}{2}(1-4u^2+4uy-y^2) \ , \qquad (5)$$

$$b(u,y) = 1 + 2ku(2u-y) + \frac{p}{2}(1+2uy-y^2) \ , \qquad (6)$$

$$c(u,y) = -(1+2ku^2+uyp) \ . \qquad (7)$$

The particle difference concentration is given by $\gamma = 2u(\rho-1) - \rho y$.

Equations (5) – (7) show that when $p \rightarrow 0$, the relevant variable is the reduced parameter $u = x/p$. When $u \ll -1$ we have $\rho \approx 1, \gamma \approx 1$. This is an A dominated regime. When $u \gg 1$ we have $\rho \approx 1, \gamma \approx -1$; a B dominated regime. In these cases the surface is covered predominantly by one of the species and is weakly reactive. The reactive zone occurs when A and B coexist, i.e., for values of x in the neighborhood of $x = 0$. The width of this zone is given by $|x/p| < 1$. The exact shape of the reaction curves and the density curves depend on the value of y. The relation $u \sim 1$ defines the width of the reactive regime. Note that for small p the total density ρ is always of the order unity.

The case of $y = \pm 1$ plays a special role because at these points one species cannot desorb at all, and the system can have an absorbing (or poisoned) state of, say, all B. The transition to this state looks like a second order phase transition [9]. The reaction rate Q may be thought of as the order parameter. This is close to the model that was investigated by Albano [8] and Zhuo and Redner [10]. (Note that in their case the desorption probability is of the order of unity: we will always consider small p.) We will discuss this case further below.

III. SPIN MODEL

A. Description

On the time scale of the reaction, for $p \ll 1$, there is a probability close to unity for an empty site to be replaced by either A or B: an empty lattice site has a short lifetime. In view of this it is natural to map the model onto a system of spin-1/2 particles on the lattice with $\uparrow \Leftrightarrow A$ and $\downarrow \Leftrightarrow B$. The dynamics of this two-state model is as follows: For each time step, a lattice site is chosen at random and desorption is tried with a probability $P^d_{A,B}$ if the site is occupied by A, B. If desorption occurs the site is then filled by A or B according to the adsorption probabilities. If no desorption occurs, a direction is chosen at random among all the nearest neighbors. If the nearest neighbor is occupied by the opposite species, then a reaction takes place. Each of the vacant sites is then replaced by a species A or B with probability P_A, P_A (here, $P_A + P_B = 1$). The order of taking desorption first and then reaction is different from other authors [2,8], as is our convention of only trying one random direction for a reaction. Both of these changes alter the simulation results only slightly, and make the theory much easier to formulate.

Let the spin variable at site i be z_i taking a value ± 1. The dynamics of this model is easily represented using a master equation. The combination of reaction and adsorption can leave a nearest neighbor pair (i, j) unchanged, flip both spins (we call this exchange), flip i (flip), or flip j (transfer). We can then write down the transition probabilities, w_E, w_F, w_T to go into the master equation:

$$\begin{aligned}
&\{z_i, z_j\} \rightarrow \{-z_i, -z_j\},\\
&\qquad w_E = (1-x^2)(1-z_iz_j)/16d\ ;\\
&\{z_i, z_j\} \rightarrow \{-z_i,\ z_j\},\\
&\qquad w_F = (1+x^2+2xz_i)(1-z_iz_j)/16d\ ;\\
&\{z_i, z_j\} \rightarrow \{\ z_i, -z_j\},\\
&\qquad w_T = (1+x^2-2xz_i)(1-z_iz_j)/16d\ . \qquad (8)
\end{aligned}$$

Desorption is governed by a transition probability w_D:

$$\begin{aligned}
&\{z_i\} \rightarrow \{-z_i\},\\
&\qquad w_D = \frac{p}{4}[1+xy+(x+y)z_i]\ . \qquad (9)
\end{aligned}$$

The master equation for configuration probability, $P\{z\}$, is

$$\begin{aligned}
\dot{P}\{z\} = &\sum_{\langle ij\rangle}\sum_{X} w_X\{z_i', z_j'\}P\{z'\} - w_X\{z_i, z_j\}P\{z\}\\
&+ \sum_i w_D\{-z_i\}P\{-z_j\} - w_D\{z_i\}P\{z_i\}\ , \qquad (10)
\end{aligned}$$

where $\langle ij\rangle$ means that i, j are nearest neighbor sites, X runs over E, F, T, and z' is the spin variable before the process occurs. From this equation we will derive a hierarchy of equations for the moments of the spin variable.

B. Moment equations

1. First moment

Using standard techniques, we calculate the equation of motion for the first moment, $\gamma_i = \sum_{\{z\}} z_i P\{z\}$. We obtain

$$\frac{d\gamma}{dt} = D\Delta_i\gamma_i - \frac{p}{2}(1+xy)\gamma_i - \frac{p}{2}(x+y) - 2xQ_i\ . \quad (11)$$

Equation (11) looks like a diffusion equation with $D = 1/2d$ an *effective* diffusion constant; Δ_i is the discrete Laplacian operator. The existence of an effective diffusion constant at a macroscopic level is somewhat unsuspected. It has the simple physical interpretation that reaction plus adsorption can effectively diffuse the spins, even in the absence of explicit diffusion. Q_i is a local reaction rate: $Q_i = D\sum_\alpha(1-\langle z_iz_{i+\alpha}\rangle)/2$, where α runs over the nearest neighbors (which can react).

After summation over the whole space we get the first moment equation for $\gamma = \sum_i \gamma_i/N$, where $Q = \sum_i Q_i/N$. We find

$$\frac{d\gamma}{dt} = -\frac{p}{2}(1+xy)\gamma - \frac{p}{2}(x+y) - 2xQ\ . \quad (12)$$

The dependence on Q couples this equation to higher moments.

2. Second moment

Similarly, we can calculate the equation of motion for the second moments $\langle z_iz_{i+k}\rangle = \sum_{\{z\}} z_iz_{i+k}P\{z\}$. We obtain the following after averaging over space and using the notation $m_k = \sum_i\langle z_iz_{i+k}\rangle/N$:

$$\begin{aligned}
\frac{dt}{dm_k} = &\ 2D\Delta_k m_k - 4DxT_k - p(1+xy)m_k - p(x+y)\gamma\\
&+[4Q+p(1+xy)+p(x+y)\gamma]\delta_{k,0}\\
&-2D(1-x^2)Q\sum_\alpha \delta_{k,\alpha}\ , \qquad (13)
\end{aligned}$$

where α again denotes the nearest neighbors. This equation contains a third order correlation function: $T_k = \sum_i\sum_\alpha\langle z_{i+k}(1-z_iz_{i+\alpha})\rangle/(2N)$. This term couples the equation for the second moment m_k to higher orders. We should note that for $x = 0$ the coupling vanishes. Our equation is an exact solution for the second moment of the spin model for any y in the case of symmetric adsorption. From the definition of the reaction rate above, we have

$$Q = D\sum_\alpha(1-m_\alpha)\Big/2. \quad (14)$$

3. Decoupling

Equations (12) – (14) do not form a closed set. In order to have a tractable set of equations, we must decouple T_k. We propose the following simple scheme:

$$DT_k = Q\gamma(1-\delta_{k,0})\ . \quad (15)$$

This ansatz assumes that Q and γ are uncoupled, and relates T to the product of a reaction rate at i and the mean population, γ, at $i+k$. The δ function takes into account the fact that $T_0 = 0$.

We now have a set of equations that couple γ, m_k, and Q. We will be interested in the steady state of the system in this paper, so we will write them down in detail only for that case.

C. Steady state

1. General solution

In the steady state, we can solve Eq. (12) for the first moment:

$$\gamma = \gamma_0 - 2xQ/\hat{p} \ , \qquad (16)$$

where $\hat{p} = p(1+xy)/2, \gamma_0 = -(x+y)/(1+xy)$. For large spatial separations, k, the second moment approaches γ^2, so that it is clearly useful to introduce $\hat{m}_k = m_k - \gamma^2$. Also, we write $\hat{Q} = Q(1-x^2)$. In terms of these changes of variables, and using the decoupling of Eq. (15) we have, in the steady state,

$$2D\Delta_k \hat{m}_k - 2\hat{p}\hat{m}_k - 2D\hat{Q}\sum_{\alpha} \delta_{k,\alpha} + 2\delta_{k,0}[2Q + \hat{p}(1-\gamma^2)] = 0. \qquad (17)$$

This equation is similar to the one that was solved in the symmetric FGZ model [3], and we use the same self-consistent method. We begin by Fourier transforming: $\sigma_q = \sum_k \hat{m}_k e^{-iqk}; \hat{m}_k = \sum_q \sigma_q e^{iqk}/N$, we can solve for σ_q:

$$\sigma_q = \hat{Q} + \frac{Q_1 + \hat{Q}(1-\hat{p}) + \hat{p}(1-\gamma^2)}{\hat{p} + 2D\sum_{j=1}^{d}[1-\cos(q_j)]} \ , \qquad (18)$$

where $Q_1 = 2(Q - \hat{Q}) = 2Qx^2$. The sum in the denominator is over the coordinate directions in d dimensions, and $q_j = \mathbf{q}\cdot\mathbf{k}_\alpha$ where $\mathbf{k}_\alpha$ are the unit vectors to nearest neighbors.

Now, σ_0 is the spatial average of $\hat{m}_k$, which in turn gives a measure of the fluctuations of the populations $N_{A,B}$. Specifically, if we define the relative fluctuation, $\Delta_{AB} = \langle (N_A - N_B)^2/N^2 \rangle$, then

$$\Delta_{AB} = \gamma^2 + \sigma_0/N = \gamma^2 + \frac{1}{N}\left(1 - \gamma^2 + \frac{(1+x^2)Q}{\hat{p}}\right) . \qquad (19)$$

This equation together with Eq. (16) and the self-consistent value of Q to be derived below can be used to estimate the anomalous fluctuations for small systems when $p \ll 1$, as in our previous work [3].

The inverse Fourier transform of Eq. (18) gives

$$m_k = \gamma^2 + [Q_1 + \hat{Q}(1-\hat{p}) + \hat{p}(1-\gamma^2)]F_d(\hat{p},k) \ ,$$
$$F_d(\hat{p},k) = \frac{1}{N}\sum_q \frac{\cos(\mathbf{q}\cdot\mathbf{k})}{\hat{p} + 2D\sum_{j=1}^{d}[1-\cos(q_j)]} \ . \qquad (20)$$

However, $m_{k=\alpha}$ is the mean number of nearest neighbors and gives the reaction rate $Q = (1-m_\alpha)/2$ [cf. Eq. (14)]. This closes the self-consistency loop and gives the central result of our analysis:

$$2Q = 1 - \gamma^2 - [Q_1 + \hat{Q}(1-\hat{p}) + (1-\gamma^2)\hat{p}]F_d \ , \qquad (21)$$

where $F_d \equiv F_d(\hat{p},\mathbf{k}_\alpha)$ for any one of the nearest neighbors, and γ is expressed in terms of Q in Eq. (16).

The behavior of F_d for small p was studied earlier [3] in cases when we can replace the sum by an integral:

$$F_d \to 1/\sqrt{2p} \qquad \text{for } d=1,$$
$$\to (1/\pi)\ln(1/p) \qquad \text{for } d=2,$$
$$\sim 1 \qquad \text{for } d=3.$$

Q is the solution of a quadratic equation, $aQ^2 + bQ + c = 0$, where the coefficients are

$$a = 4x^2(1-\hat{p}F_d)/\hat{p}^2,$$
$$b = 2 - 4x\gamma_0/\hat{p} + [2x^2 + (1-x^2)(1-\hat{p}) + 4\gamma_0 x]F_d,$$
$$c = -(1-\gamma_0^2)(1-\hat{p}F_d), \qquad (22)$$

where γ_0 is given in Eq. (16). One can check that the discriminant of the quadratic equation is always positive. We are physically constrained to choose the root of the quadratic such that $Q \geq 0$, which is unique unless $c = 0$. This, however, is an interesting special case that occurs for $\gamma_0^2 = 1$, i.e., $y = \pm 1$. In this case a trivial poisoned state exists for every value of x. Because $c = 0, Q = 0$ is always a solution to the equation, and for a range of x there is another. We will return to this case below.

2. Unique reactive solution

Now consider the solution for small p when $y \neq \pm 1$. This means that we have a unique reactive steady state. In the limit $p \ll 1$ and for small x we have

$$a \approx \frac{4x^2}{\hat{p}^2} \ ,$$
$$b \approx F_d - \frac{4x\gamma_0}{\hat{p}} \ ,$$
$$c \approx -(1-\gamma_0^2). \qquad (23)$$

We will show here that the reactive zone, i.e., the transition zone between A dominated and B dominated systems, is of order $\hat{p}F_d(\hat{p}) \sim \sqrt{p}$ for $d = 1$, and $\sim p\ln(1/p)$ for $d = 2$. Thus for $d < 3$ this transition zone is quite different from the mean-field predictions that give a width of order p.

This is most easily done by defining $x^* = x/\hat{p}F_d(\hat{p})$. In Eq. (23) we see that $a \sim F_d^2, b \sim F_d, c \sim 1$. Then we find that QF_d is a function of x^* alone:

$$QF_d = \left[-m + \sqrt{m^2 + 16[x^*]^2(1-\gamma_0)}\right]/8[x^*]^2 \ ,$$
$$m = 1 - 4x^*\gamma_0. \qquad (24)$$

If we can expand the square root, $|b| \gg \sqrt{-4ac}$ we have for $m > 0$

$$Q \approx \frac{1-\gamma_0^2}{F_d} \sim \begin{cases} (1-\gamma_0^2)\sqrt{p}, & d=1 \\ (1-\gamma_0^2)/\ln(1/p), & d=2, \end{cases} \qquad (25)$$

and for $m < 0$

$$Q \approx -\frac{F_d m}{8[x^*]^2}. \qquad (26)$$

The peak of the curve occurs for the latter case for $y \approx$

-1, a case we will study in the next section.

We will not pursue the study of finite lattice size effects, mentioned above [cf. Eq (19)] the so-called fluctuation dominated kinetics. To do so it is only necessary to consider the L dependence of F_d when we do not replace the sum by an integral [3,4]. This manifests itself in a bimodal distribution of γ.

We should note that the dependence of the reaction rate on p is an indication of the segregation of the system of domains rich in A or B [3,11]. In the case where neither of the species is particularly in excess (the reactive regime), there is a domain size Λ such that $Q \approx \rho_A \rho_B/\Lambda$. From Eq. (25) we have $\Lambda \gg 1$. This reduction in reaction rate due to segregation is exactly the kind of effect that MF approaches are unable to reproduce. In the section on simualations, below, we explicitly demonstrate the onset of segregation.

3. Absorbing solution

Now we consider the special case of $y = -1$. This seems to correspond to having a Schlögl transition to an absorbing (A poisoned) state. Here we have $\gamma_0 = 1$ and $c = 0$ and two possible solutions: $Q = -b/a, Q = 0$. Since $a > 0$ for $b < 0$, we have a possible reacting steady state. We have shown this to be a stable attractor of the kinetics by linearizing the time-dependent equations around this state. There are no growing solutions since the eigenvalues of the linear operator are negative.

For $b > 0$ the only stable attractor of the kinetics is the solution $Q = 0$, which means that the whole lattice is covered with A. This transition from a reactive state to a nonreactive state is what we identify as a continuous phase transition as a function of the transition parameter x, with the reaction rate Q as the order parameter. In the limit of an infinite lattice the critical point x_c is the solution of the equation $b(x,p) = 0$. In the limit of small p this gives a $x_c \approx \hat{p}F_d/4$ and $Q \approx p(x - x_c)/x_c^2$.

Thus for $d = 1$ we have $x_c = \sqrt{p}/8, Q^* = Q/\sqrt{p} \sim (x^* - x_c^*)$, where $x^* = x/\sqrt{p}$, as above, is the natural dimensionless control parameter, and $x_c^* = 1/8$. In a like manner, for $d = 2$ we can put $x_c = p\ln(1/p)/8\pi, x^* = 2\pi x/[p\ln(1/p)]$ and $Q^* = Q\ln(1/p) \sim (x^* - x_c^*)$.

If we compare to the naive MF above, we have two additional features in $d = 1, 2$. The transition is shifted,

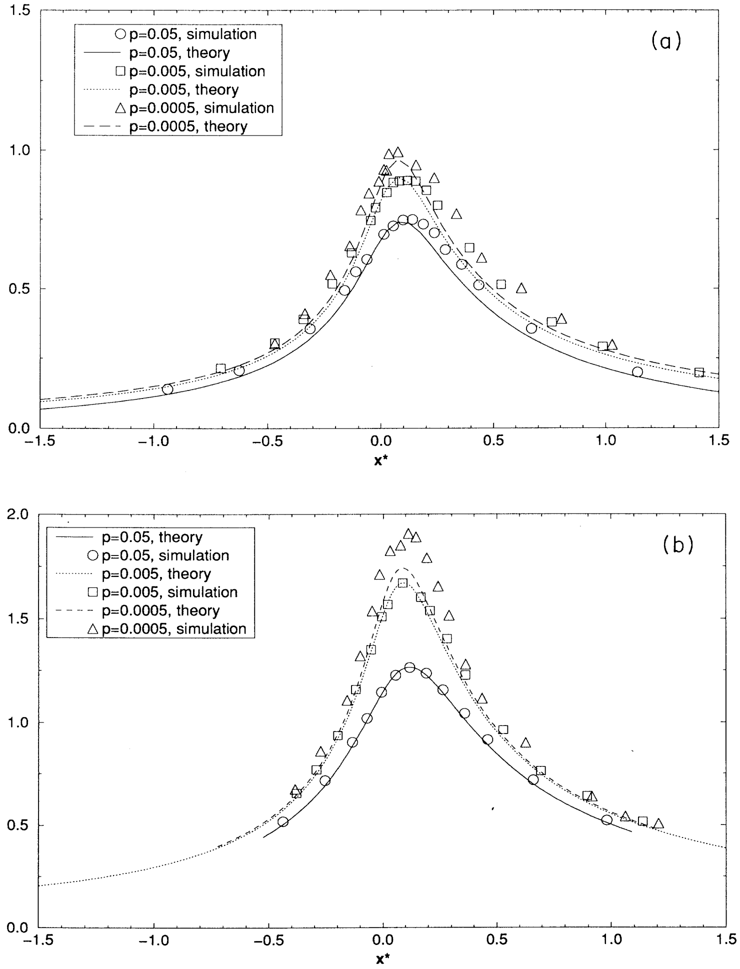

FIG. 1. (a) Monte Carlo simulation results for the scaled reaction rate in the spin model, $d = 1$. We plot $Q^* = Q/\sqrt{\hat{p}}$ versus $x^* = x/\sqrt{\hat{p}}$ for $y = -0.3$, and $p = 0.05, 0.005, 0.0005$, and compare to the decoupling approximation. (b) Monte Carlo simulation results for scaled reaction rate in the spin model, $d = 2$. We plot $Q^* = Q\ln(1/\hat{p})$ versus $x^* = x/\hat{p}\ln(1/\hat{p})$ for $y = -0.3$, and $p = 0.05, 0.005, 0.0005$, and compare to the decoupling approximation.

and the width of the transition zone depends on the desorption probability and on the spatial dimension in an unusual way, as above. These features do not occur in the usual Schlögl model, and correspond to taking a certain class of correlations and fluctuations into account. Nevertheless, in all dimensions, the exponent β for the dependence of the order parameter on u is still 1. Our theory is a mean-field theory for the phase transition and misses the critical fluctuations [13]. Thus, very near the transition we expect, and do find in simulations, clusters of the minority species which grow for a time and ultimately die, and whose distribution of survival times has a long tail.

D. Generalization to fractal substrates

It is possible to give a detailed argument to generalize our theory to a fractal structure. This is presented in detail in a recent article by Clément *et al.* [4], in the particular case of a symmetric FGZ model and tested on percolation clusters. A discussion on the possible limits of this approach is presented as well. Here it will suffice to use heuristic approach since we know the origin of nonclassical behavior for models of this type. These are a consequence either of spatial organization of reactants on a substrate due to incomplete mixing—the segregation we have been discussing, or finite size effects where the reaction kinetics is fluctuation dominated [3]. In this last case the topology of the substrate seems irrelevant. Here we focus on segregation.

A study on catalytic models on fractals can be found in Ref. [11]. We can try to understand the situation by proposing that in Eq.(25), the function F_d should be replaced by a function $F_{d_s}(p)$, where d_s is the spectral dimension of the lattice [3]. To be consistent with the formalism above, we must define F_{d_s} in such a way that when $p \to 0$, F_{d_s} goes as $p^{d_s/2-1}$. Thus, we think that we can distinguish two regimes corresponding to the value of $x^* = x/p^{d_s/2}$. When $|x^*| \gg 1$ our fractal will be covered with one or the other species, and when $|x^*| < 1$ the system should be reactive. Proceeding by analogy, we guess that $Q \sim p^{1-d_s/2}$ and that there is segregation up to a scale $\Lambda \sim p^{d_s/2-1}$. We will test this prediction below.

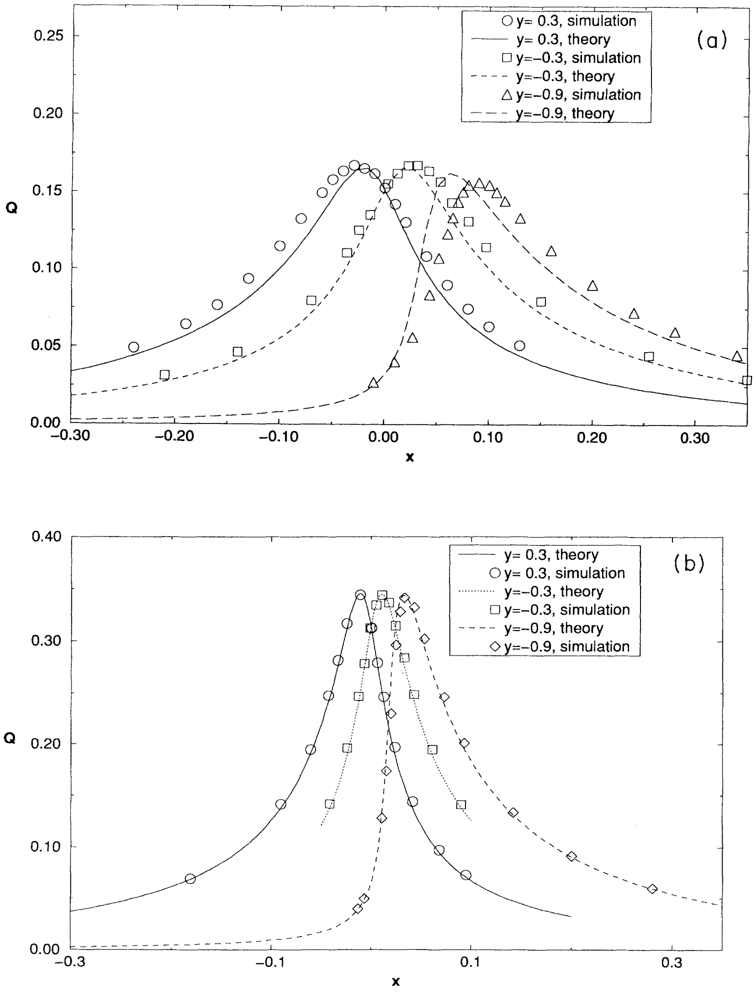

FIG. 2. (a) Monte Carlo simulation results for the reaction rate Q in the spin model, $d = 1$ for $y = 0.3, -0.3, -0.9$, and $p = 0.05$ compared to the decoupling theory. (b) Monte Carlo simulation results for the reaction rate Q in the spin model, $d = 2$ for $y = 0.3, -0.3, -0.9$, and $p = 0.05$ compared to the decoupling theory.

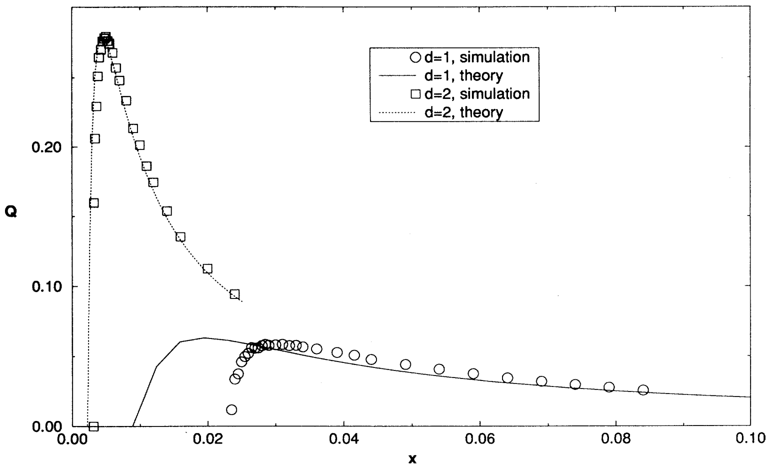

FIG. 3. Monte Carlo simulation results for the reaction rate Q in the spin model, $d = 1, 2$ for $y = -1$, and $p = 0.005$ compared to the decoupling theory.

IV. MONTE CARLO SIMULATIONS

In the foregoing the two-state model was solved analytically using decoupling. The validity of the scheme can be tested directly by performing a series of Monte Carlo (MC) simulations of the spin model. This we will do in various cases. However, there is another sort of simulation: if p is small enough, we should be able to go back to the full reaction model of the second section, and show that we have a reasonable account. We present simulations of this sort as well.

The algorithm describing the reaction model goes as follows: a site is chosen at random; if this site is empty a landing trial of A or B is attempted with relative weight $P_{A,B}$. If the site is not empty a desorption trial is attempted with a probability $P^d_{A,B}$ depending on the occupation. If no desorption occurs, a direction is chosen at random. A reaction occurs if the chosen nearest neighbor is of the opposite species. Of course, in this case, the lattice is not full, and if there are many vacancies, we cannot expect any agreement with our theory. Nevertheless, the general scaling structure of the densities $\rho_{A,B}(x)$ and the reaction rate $Q(x)$ can be tested.

Simulations of the spin model were made on three types of substrate: (i) a one-dimensional (1D) chain of sites, (ii) a square surface, and (iii) a percolation cluster at the percolation threshold. Periodic boundary conditions were used and the number of sites was chosen to be about the same in the three instances. We chose the simulation conditions so that $p \ll 1$ but not so small that we get large fluctuations due to finite-size effects [3]. In 1D this amounts to having $L \gg 1/\sqrt{p}$.

In Fig. 1(a) we take $y = -0.3$ and for various p and plot $Q(x)$ for 1D systems, and similarly in Fig. 2(b) for 2D. The solid lines are the predictions of the decoupling theory. In order to show the scaling, we have, in fact, plotted $Q^* = Q/\sqrt{p}$ as a function of $x^* = x/\sqrt{p}$ in 1D and $Q^* = Q\ln(1/\hat{p})$ as a function of $x^* = x/[\hat{p}\ln(1/\hat{p})]$ in 2D.

In Figs. 2(a) and 2(b) we give the reaction rate, Q, as a function of x for various y. A progressive skewing from a symmetric curve to the second order transition curve is clearly seen. A direct comparison is made with the

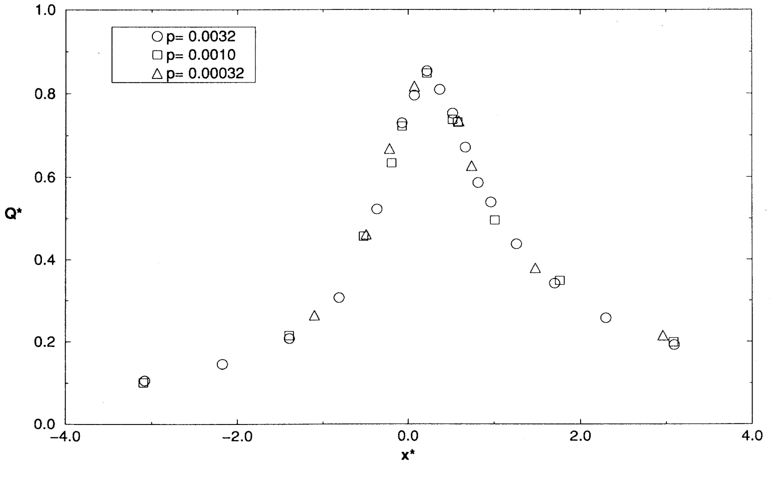

FIG. 4. Rescaled reaction rate on an incipient percolation cluster in 2D for $y = -0.3$. We plot $Q^* = Qp^{d_s/2-1}$ as a function of $x^{-d_s/2}$, for $p = 0.0032, 0.00010, 0.000032$.

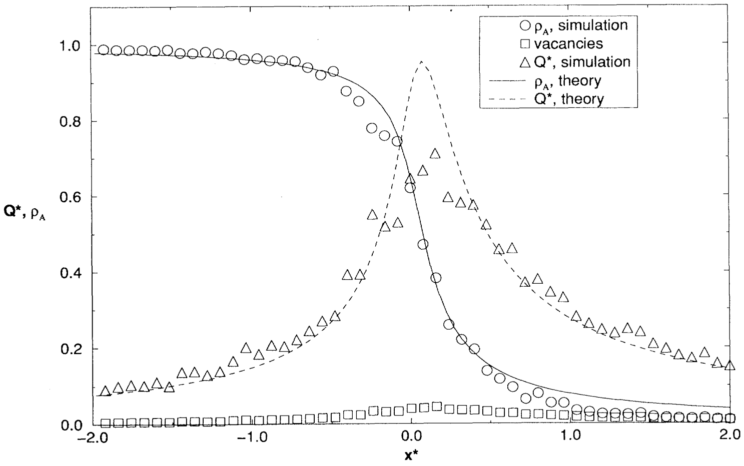

FIG. 5. Monte Carlo simulation results for the reaction model, $d = 1$. We plot $Q^* = Q/\sqrt{p}$ and ρ_A versus $x^* = x/\sqrt{p}$ for $y = -0.3$, and $p = 0.001$, and compare to the decoupling approximation. The density of vacancies, also shown, is quite small for this p.

analysis (solid lines). The scaling behavior is reasonably reproduced. For $y = -1$ and $d = 1$ (Fig. 3) we do not find particularly good agreement between the spin model simulations and the decoupling theory in the immediate vicinity of the transition. This is due to the critical fluctuations that occur on scales larger than those we can treat. In 2D the agreement is surprisingly good.

In Fig. 4, we show Q for a spanning percolation cluster for $y = -0.3$ for various p. In order to test the scaling predictions we have plotted $Qp^{d_s/2-1}$ as a function of $xp^{-d_s/2}$. We took the value $d_s = 4/3$. Our ansatz for the fractal scaling is quite well obeyed.

In Fig. 5 we show the results of the reaction model for 1D for $p = 0.001$ in the form of a scaling plot. We find good agreement with our decoupling theory, except for a small region near the peak of the reaction-rate curve (where there are the largest number of vacancies). The width of the transition region $\sim \sqrt{p}$ is well reproduced by the decoupling theory, whereas MF would predict a transition zone $\sim p$, namely about 30 times smaller.

In Fig. 6 we show a histogram of the distribution of A and B domain sizes (weighted by the number of sites) for $d = 1, p = 0.05, y = -0.9$. These data clearly display self-organization: the distributions are quite different, with a maximum for the B domains and a broad tail for the A domains. This accounts for the departure of Q from mean-field behavior.

V. DISCUSSION AND CONCLUSIONS

We have studied a model for catalysis of the form $A + B \to 0$ in the case where the fast time scales are adsorption and the reaction between species. Our calculation uses a two-state spin model which we decouple at the level of three-particle correlations. We address the issue of spatial self-organization. Our solution gives overall behavior that is qualitatively similar to MF theory (transitions between saturated domains in A or B, second order transition, etc.), but there is strong quantitative disagreement between the two. We find that the width in x of the transition zone is much larger in the spin model and this trend increases in lower dimension. The reaction rate depends on the desorption probability in a completely different way than in MF. It is much smaller due to a spatial segregation effect. This segregation is already present in the original FGZ model, where the role of the two species was symmetric. We gave scaling arguments to extend our scaling arguments to a fractal structure.

Our refined theory gave a reasonable account of the continuous transition to a poisoned state when one species cannot desorb, though without critical fluctuations, of course. We show again that the width of reaction transition is affected by the desorption probability of the other species. We presume that the critical behavior of our model is the same as others with one absorbing state [12] but we have not yet checked this by direct simulation, and it would be of some interest to do so.

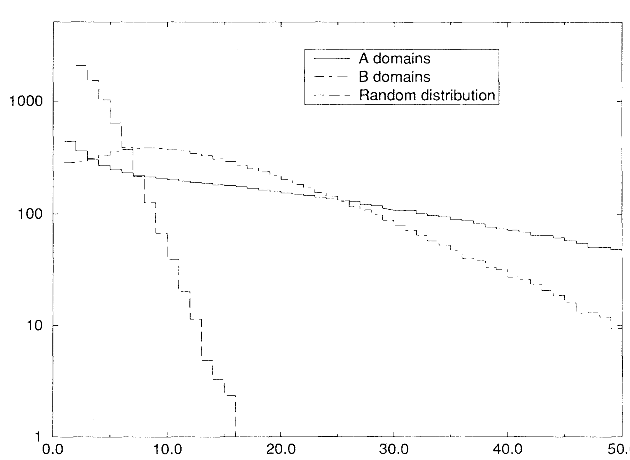

FIG. 6. Self-organization of the reactants illustrated with the first moment, $zn(z)$ of the domain size distribution $n(z)$ as a function of the size z for $L = 16\,384, p = 0.05, y = -0.9$. We choose x so that $\rho_A = \rho_B$.

ACKNOWLEDGMENTS

We would like to thank R. M. Ziff, C. Caroli, and C. Aslangul for interesting discussions. L.M.S. is supported by the U.S. Department of Energy, Grant Nos. DE-FG02-85ER5418 and DE-FG02-95ER45546. We were supported by NATO collaborative Grant No. CRG910897. The Laboratoire d'Acoustique et d'Optique et de la Matière Condensée and the Groupe de Physique du Solide are URA's of the CNRS.

[1] R. Ziff, E. Gulari, and Y. Barshad, Phys. Rev. Lett. **56**, 2553 (1986).

[2] K. Fichthorn, I. Gulari, and R. Ziff, Phys. Rev. Lett. **63**, 1527 (1989).

[3] E. Clément, P. Leroux-Hugon, and L. Sander, Phys. Rev. Lett. **67**, 1661 (1991); J. Stat. Phys. **65**, 925 (1991).

[4] E. Clément, P. Leroux-Hugon, and P. Argyrakis, Phys. Rev. E **49**, 4857 (1994).

[5] P. L. Kapivski, Phys. Rev. A **45**, 1067 (1992).

[6] C. Flament, E. Clément, P. Leroux-Hugon, and L. Sander, J. Phys. A **25**, L1317 (1992).

[7] J. W. Evans and T. R. Ray, Phys. Rev. E **47**, 1018 (1993).

[8] E. V. Albano, Phys. Rev. Lett. **69**, 656 (1992); Phys. Rev. A **46**, 5020 (1992); Phys. Rev. Lett. **72**, 108 (1994).

[9] F. Schlögl, Z. Phys. **253**, 147 (1972).

[10] J. Zhuo and S. Redner, Phys. Rev. Lett. **70**, 2822 (1993).

[11] E. Clément, P. Leroux-Hugon, L. Sander, and P. Argyrakis, J. Phys. Chem. **98**, 7274 (1994).

[12] H. K. Janssen, Z. Phys. B **42**, 151 (1981); P. Grassberger, *ibid.* **47**, 465 (1982).

[13] P. Grassberger and A. de la Torre, Ann. Phys. (N.Y.) **122**, 373 (1979).